The effects of uniform temperature and bolts fracture on the behaviour of high strength bolted frictional steel connection in Dashegnguan Railway Bridge

Gaoxin Wang* and Youliang Ding**

*State Key Laboratory for Geomechanics & Deep Underground Engineering, China University of Mining and Technology, Xuzhou 221116, China
**The Key Laboratory of Concrete and Prestressed Concrete Structures of Ministry of Education, Southeast University, Nanjing 210096, China
*Corresponding Author: civilgxwangg@hotmail.com

ABSTRACT

For the friction-type high-strength bolted joint, the bolt fracture can cause redistribution of interface friction, which can seriously endanger the connection safety of structural members. However, current studies barely focus on the redistribution of interface friction after bolt fracture. Therefore, this paper will specifically carry out finite element analysis on the redistribution of interface friction caused by fractured bolts. Firstly, the refined finite element model of friction-type high-strength bolted joint is used to investigate the variation of interface friction under uniform temperature as well as the distribution of interface friction in different areas. Furthermore, random selection method is introduced to explain how the quantity and location of fractured bolts influence the redistribution of interface friction. Finally, the mathematical model of friction redistribution is built to describe the redistribution of interface friction in the high-strength bolted frictional steel connection after bolt fracture. After validation, the mathematical model can well describe the redistribution of interface friction caused by fractured bolts, which can provide useful reference for the frictional steel connection design of high strength bolts.

Keywords: Friction-type high-strength bolt; interface friction; bolt fracture; uniform temperature; friction steel connection.

INTRODUCTION

Nowadays, the friction-type high-strength bolts have been widely used in the joint connection of steel structures (Bednarz & Zhu, 2014; Chul & Shirley, 2015; Ju & Oh, 2016). For the friction-type high-strength bolted joint, the interface friction in the contact surfaces of splice plates can transfer the internal forces in the structural members, which plays one important role in the connection of different structural members. However, some friction-type high-strength bolts are inevitably fractured under complex service environment. For example, from December 2010 to March 2016, a total of 277 friction-type high-strength bolts were fractured in the Dashegnguan Railway Bridge as shown in Figure 1, and such bolt fracture is happening every year. Bolt fracture can result in the redistribution of interface friction, which may decrease the shear-resistant capacity of interface friction and endanger the connection safety of structural members.

Figure 1. One fractured friction-type high-strength bolt.

Therefore, it is significant to thoroughly study the effect of bolt fracture on the redistribution of interface friction. What should be mentioned is that the interface friction cannot be easily monitored and collected at bridge site, so finite element simulation is one effective procedure to simulate the interface friction under environmental loads. Moreover, the environmental loads are very complex, including temperature field, wind field, and train load. For the Dashengguan Railway Bridge, some relevant studies have revealed that this bridge is mainly subjected to the uniform temperature field from 0 a.m. to 6 a.m. at night (Wang & Ding, 2015; Ding *et al.*, 2017), and the time history of the uniform temperature from March 2013 to November 2013 shows obvious seasonal characteristics, as shown in Figure 2. Therefore, uniform temperature is one type of simple but non-negligible environmental load, and this paper specifically will carry out the finite element analysis on the redistribution of interface friction under uniform temperature field from the Dashengguan Railway Bridge.
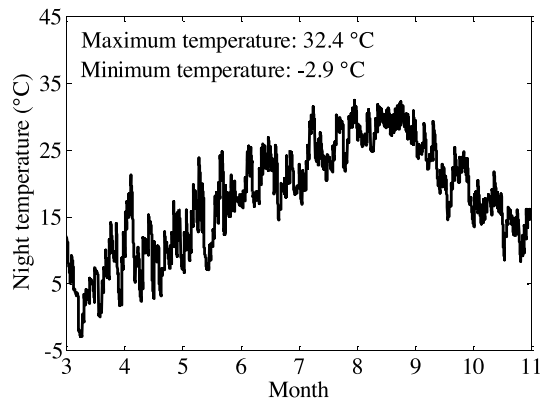
Figure 2. The variation of uniform temperature field from March 2013 to November 2013.

In detail, the redistribution of interface friction caused by bolt fracture and uniform temperature is thoroughly investigated using one whole bridge finite element model associated with one refined friction-type high-strength bolted joint. The random selection method is introduced to reveal how the quantity and location of fractured bolts influence the redistribution of interface friction. And furthermore, considering that few studies have focused on the redistribution of interface friction after bolt fracture under uniform temperature field, one mathematical model is built using data-driven method to describe the redistribution of interface friction in the friction-type high-strength bolted joint after bolt fracture, which can provide useful reference for the frictional steel connection design of high strength bolts. With regard to the data-driven method, some mathematical functions such as linear equation and Fourier Series can be used to fit the simulated data from the bridge finite element model, which has been commonly used in current research (Delgado *et al.*, 2018; Song *et al.*, 2018).

LITERATURE REVIEW

At present, many researchers have carried out experimental and numerical studies on the mechanical and fatigue performance of friction-type high-strength bolted joints (Ali *et al.*, 2012; Carlos *et al.*, 2017; Chakherlou et al., 2013; Janne *et al.*, 2016). For example, Carlos *et al.* (2017) carried out the investigation on the fretting fatigue failure mechanism of bolted joints in high-strength steel subjected to different levels of pre-tension; Ali *et al.* (2012) studied the effect of contact forces on fretting fatigue behavior of bolted plates. However, these studies barely focus on the redistribution of interface friction after bolt fracture, and furthermore, these studies have not revealed how the quantity and location of fractured bolts influence the redistribution of interface friction. As mentioned earlier, the redistribution of interface friction may decrease the shear-resistant capacity of interface friction and endanger the connection safety of structural members, so it is meaningful to carry out deep research on the redistribution of interface friction after bolt fracture.

FINITE ELEMENT MODELLING

In this section, in order to investigate the redistribution of interface friction caused by uniform temperature and bolt fracture, one whole bridge model for the Dashengguan Railway Bridge associated with one refined bolted joint model is concretely illustrated based on the finite element software LSDYNA.

Description of the Dashengguan Railway Bridge

The Dashengguan Railway Bridge is designed as the river-crossing channel for Beijing-Shanghai high-speed railway lines. Its main girder is one continuous steel truss arch girder and its main span is 336 m, as shown in Figure 3. The continuous steel truss arch girder is composed of multiple structural members, such as top chord members, bottom chord members, deck chord members, diagonal web members, suspender members, horizontal bracing members, vertical bracing members, and steel bridge deck, which are made of Q370qE steel (i.e., the tensile strength is 490 MPa and the yield strength is 330 MPa). These structural members are connected by friction-type high-strength bolts and splice plates. For the friction-type high-strength bolts, its material is made of 35VB steel, its dimension is M30 (i.e., the diameter of bolt screw is the 30 mm), and its mechanical performance is 10.9s (i.e., the tensile strength is 1040 MPa~1240 MPa and the yield strength is 940 MPa) (GB/T 1231-2006, 2006); for the splice plates, its material is made of Q420qE steel (i.e., the tensile strength is 550 MPa and the yield strength is 410 MPa). There are seven supports (A~G) as shown in Figure 3, where support D is fixed and the other supports can allow free horizontal expansion of main girder in the longitudinal direction.

Beside, for the steel truss members, the thickness, Young's modulus, shear modulus, density, Poisson's ratio, and thermal expansion coefficient are 36 mm~48 mm, 205.9 GPa, 79.2 GPa, 7853 kg/m^3, 0.3, and 0.000013/°C, respectively; for the friction-type high-strength bolts, Young's modulus, shear modulus, density, Poisson's ratio, and thermal expansion coefficient are 206 GPa, 79.38 GPa, 7820 kg/m^3, 0.28, and 0.0000125/°C, respectively; for the splice plates, the thickness, Young's modulus, shear modulus, density, Poisson's ratio, and thermal expansion coefficient are 18 mm~20 mm, 206 GPa, 79.38 GPa, 7850 kg/m^3, 0.28, and 0.000013/°C, respectively.
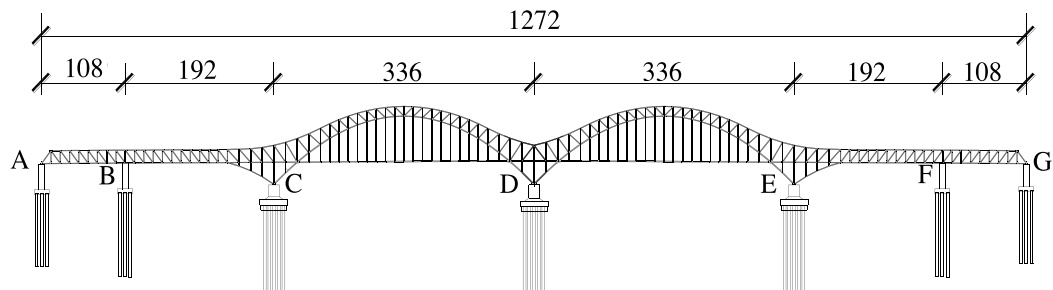
Figure 3. The design drawing of the Dashenggugan Railway Bridge (unit: m).

The whole bridge model

By referring to the design drawing of the Dashengguan Railway Bridge, the whole bridge is modeled using the computer software LSDYNA as shown in Figure 4 (Ding *et al.*, 2017). In this model, all the top chord members (except the top chord member P_1P_2), bottom chord members, deck chord members, diagonal web members, suspender members, horizontal bracing members, and vertical bracing members are modeled by Belytschko-Schwer resultant beam elements, and each beam element contains two six-degree-of-freedom nodes; the steel bridge deck is modeled by Belytschko-Lin-Tsay shell elements, and each shell element contains four six-degree-of-freedom nodes. All the friction-type high-strength bolted joints in the truss members except the top chord member P_1P_2 are simplified as rigid joints. Support D is constrained in all three translational directions, while supports A, B, C, E, F, and G are constrained in the Z-translational and Y-translational directions and are free to move in the X-translational direction.
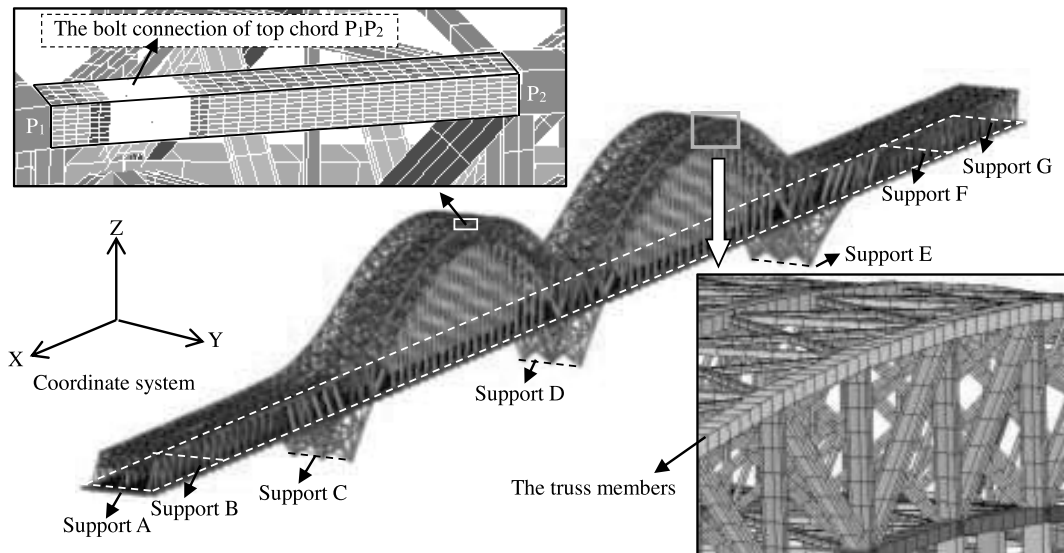
**Figure 4.** The whole bridge model using LSDYNA.

The bolted joint model

In addition to the whole bridge model, the friction-type high-strength bolted joint in the top chord member P_1P_2 is specifically modeled as shown in Figure 5. This bolted joint has the box-shaped cross section and contains 24 splice plates and 728 friction-type high-strength hexagonal bolts, as shown in Figure 5. In this bolted joint model, each friction-type high-strength bolt consists of four parts: bolt screw, bolt nut, and two plain washers. The steel plates of top chord member P_1P_2, the splice plates, and the plain washers are modeled by Belytschko-Lin-Tsay shell elements, and the bolt screws and nuts are modeled by constant stress solid elements, and each solid element contains eight three-degree-of-freedom nodes. The whole bridge model and bolted joint model are connected together by, respectively, coupling the boundary nodes at points P_1 and P_2.
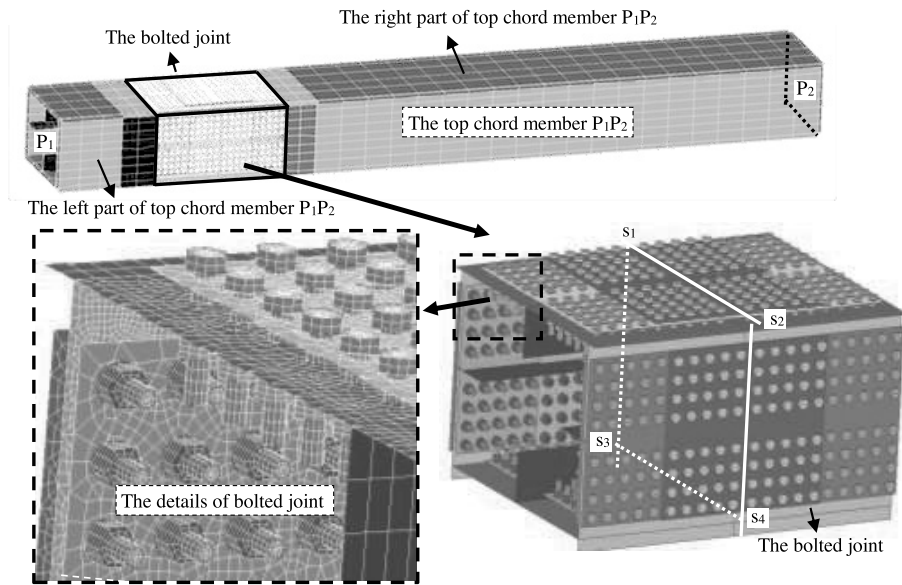
Figure 5. The bolted joint model using LSDYNA.

In detail, the 24 splice plates are uniformly distributed at four sides of the box-shaped cross section of top chord member P_1P_2 (i.e., each side contains 6 splice plates), as shown in Fig. 6(a). Each splice plate symmetrically connects the left part and right part of top chord member P_1P_2 together, and the symmetric axes are lines S_1S_2, S_1S_3, S_2S_4, and S_3S_4, as shown in Figure 5. According to the anti-sliding mechanical experiment in the design drawing of the Dashengguan Railway Bridge, the static friction coefficient of contact interface between splice plates is 0.45. Besides, the friction-type high-strength hexagonal bolt is shown in Fig. 6(b), which is preloaded with the clamping force 355 kN. Specifically, one vector defining the direction normal to the cross section of bolts is employed in the friction connection, which can quickly initialize the clamping force in the solid elements normal to the cross-section plane of bolts.
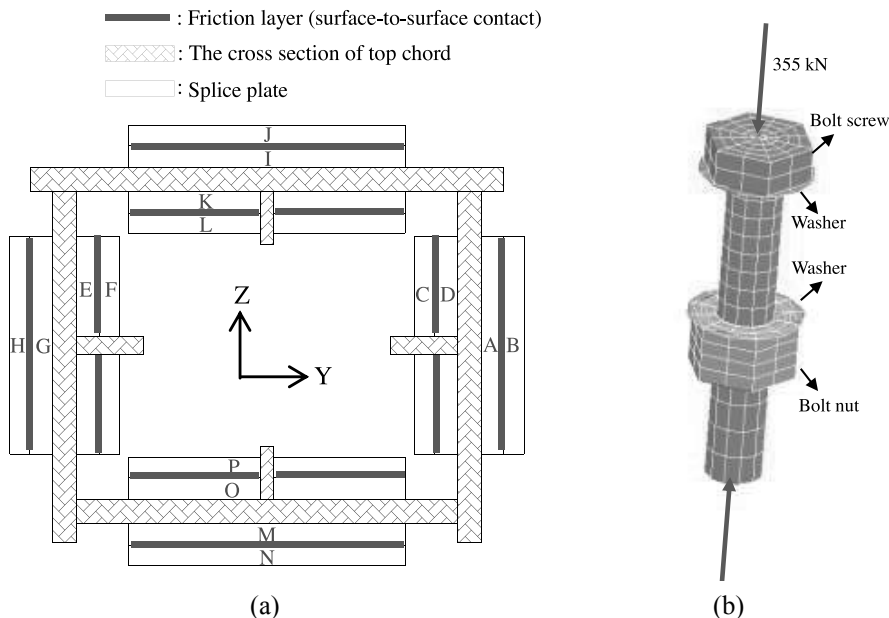
Figure 6. The details of splice plates and friction-type high-strength bolts. (a) Front view of the multi-layer splice plates; (b) the friction-type high-strength bolt.

The splice plates, bolts, and top chord member interact with each other through their contact interfaces. The contact interface in the bolted joint is simulated using the "automatic-surface-to-surface-smooth" contact type in the LSDYNA software, which can effectively transfer the change of normal interface force and shear interface force caused by temperature and bolts fracture from one splice plate to another splice plate through calculating the automatic surface-to-surface contact algorithm in LSDYNA software. The von Mises stresses in the bolted joint caused by clamping force are shown in Figure 7, including the stresses in the whole bolted joint, one bolt, and the left-side interface surfaces of plates A and B. It can be seen that the pressures on the contact surfaces caused by clamping force can be effectively transferred from one splice plate to another by comparison of Figs. 7(c) and 7(d).


(a)

(b)

(c)

(d)
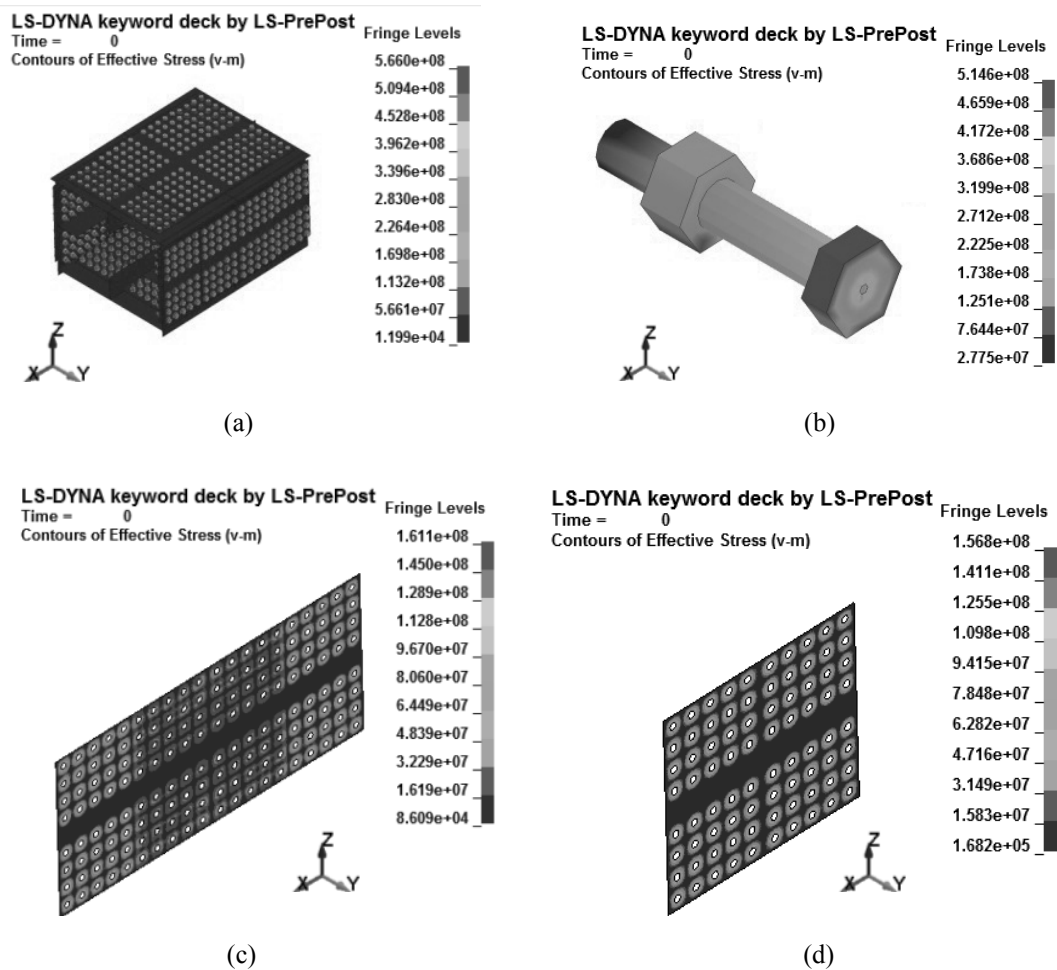
Figure 7. The von Mises stresses in the bolted joint caused by the clamping force (Unite: Pa). (a) The stress in the whole bolted joint; (b) The stress in one bolt; (c) The stress in the left-side surface of plate A; (d) The stress in the left-side surface of plate B.

Model validation

The interface friction is hardly monitored and collected from bridge site to validate the finite element model. But considering that the interface friction is used to transfer the internal forces in the truss members, the monitoring strain data under uniform temperature field is employed to validate the finite element model instead of interface friction data. Specifically, if the interface friction can well transfer the internal forces in the truss members, the simulated strain should coincide with the monitoring strain under the same uniform temperature. Therefore, two strain sensors

are placed on the top chord member P_1P_2 (Ding *et al.*, 2017), and the average strain of two strain sensors is calculated from March 2013 to November 2013, as shown in Figure 8. Moreover, the uniform temperature field in Figure 2 is loaded on the finite element model to simulate the strain in the top chord member P_1P_2, as shown in Figure 8. Usually, the monitoring and simulated strains do not have the same initial values, so the monitoring strain in Figure 8 has been offset to have the same initial value with simulated strain before validation. By comparison, it can be seen that the monitoring and simulated strains have the similar trends, verifying that the modeled bolted joint can well transfer the internal force in the top chord member P_1P_2.
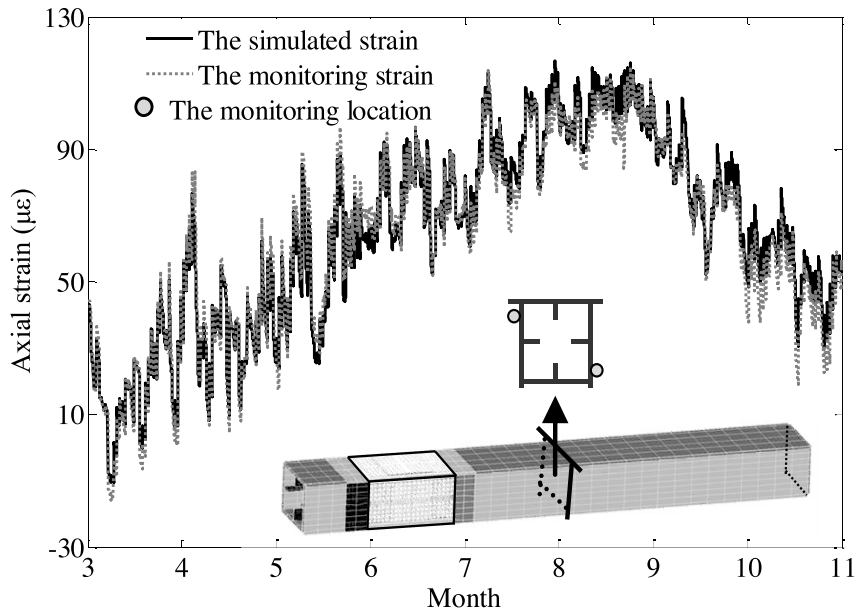
Figure 8. The monitoring and simulated strains.

THE EFFECT OF UNIFORM TEMPERATURE

In this section, the effect of uniform temperature on the behaviour of high-strength bolted frictional steel connection is deeply studied, including the variation of interface friction with temperature as well as the distribution of interface friction in different areas.

Variation of interface friction with temperature

The uniform temperature field in the whole finite element model is loaded from 0 °C to 20 °C and increases 4 °C at every time step. The uniform temperature field can cause interface friction in the contact surfaces of splice plates. Relevant research has shown that the top chord member is mainly subjected to axial internal force under uniform temperature field (Ding *et al.*, 2017), so herein the interface friction in the X direction from the left symmetric part of splice plate A is mainly studied, as shown in Figure 9.

In order to investigate the distribution of interface friction in the splice plate A, the splice plate A is divided into 10 areas from S_1 to S_{10}. What should be mentioned here is that each element in each divided area has two contact surfaces, and each contact surface contains the interface friction, so the interface frictions in the two contact surfaces should be summed together to obtain the total interface friction of each element. Furthermore, the interface friction in the divided area S_i is calculated by summing together all the interface frictions of the elements in the divided area S_i, where i denotes the serial number of divided area, and i=1, 2, 3, …, 10. According to the inspection results of fractured bolts in the Dashengguan Railway Bridge (Jin, 2013), the locations of fractured bolts are random and there are no certain areas for bolt fracture because of complex influence factors.
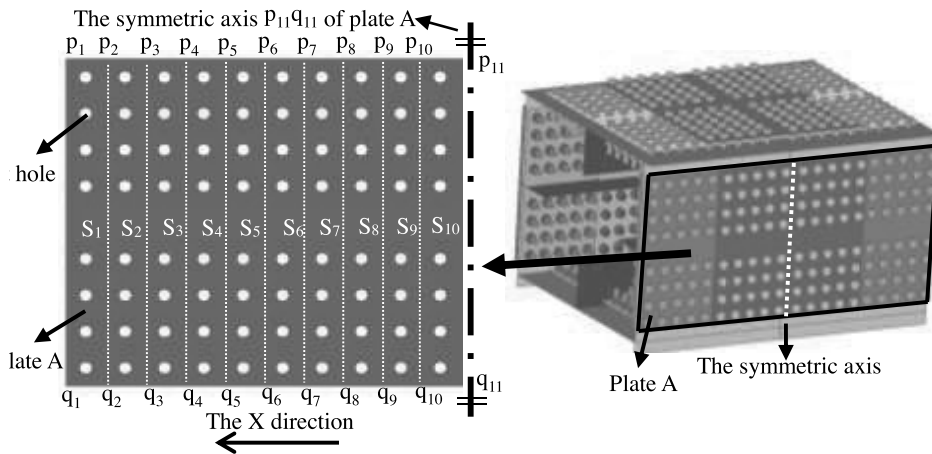
Figure 9. The divided areas of left symmetric part of plate A.

Finally, the interface friction in each area S_i is calculated at every time step through static implicit analysis. For example, the variation of interface friction with increasing temperature in the area S_{10} is shown in Figure 10, showing obvious linear characteristics. Therefore, it is further fitted by one linear equation as follows:

$$f(S_{10}, T)=k(S_{10})T+c(S_{10}) \tag{1}$$

where $f(S_{10}, T)$ denotes the interface friction in the area S_{10} caused by increasing temperature T; $k(S_{10})$ and $c(S_{10})$ denote the linear slope and constant term of linear equation in the area S_{10}, respectively. Linear slope means the variation of interface friction with temperature. After fitting the linear equation using least square method (Xiao & Tong, 2012), the estimated values of $k(S_{10})$ and $c(S_{10})$ are 2.43 and 0.12, respectively. The value of $k(S_{10})$ means that the interface friction in the area S_{10} will linearly increase 2.43 kN as temperature increases 1 °C.

Many research results have verified that the temperature-induced effects (such as strain and displacement) have linear correlation with temperature field (Ding *et al.*, 2017; Wang *et al.*, 2016), and here the interface friction also has linear correlation with temperature as shown in Figure 10. Moreover, the linear slope indicates the sensitivity of interface friction in the steel connection to the temperature increase, and higher linear slope in the area S_i means higher interface friction in the area S_i. Besides, the linear slope relates to the shear capacity provided by group bolts, and higher linear slope in the area S_i means that the interface friction is closer to the shear capacity of group bolts in the area S_i.
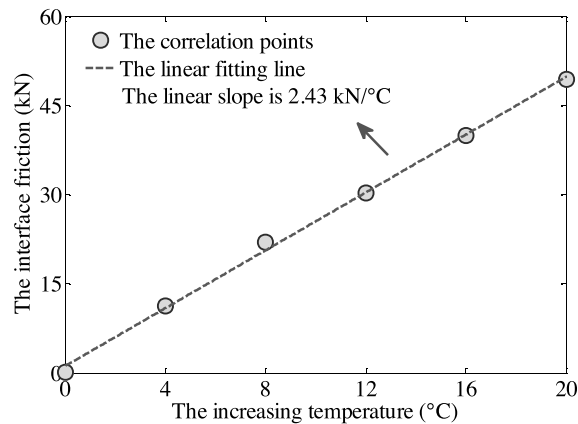

**Figure 10.** The variation of interface friction with increasing temperature in the area S_{10}.

Distribution of interface friction in different areas

After analyzing the variation of interface friction with increasing temperature in the area S_{10}, the interface frictions in the other areas $S_1 \sim S_9$ also have good linear correlation with uniform temperature field, and their linear slopes $k(S_i)$ and constant terms $c(S_i)$ in the area S_i are estimated using least square method, as shown in Figs. 11(a) and 11(b), respectively. It can be seen that all the linear slopes in the 10 areas are positive, indicating that increasing temperature can result in increasing interface friction. Additionally, the linear slopes gradually decrease from S_1 (2.35 kN/°C) to S_7 (0.83 kN/°C), and then gradually increase from S_7 (0.83 kN/°C) to S_{10} (2.43 kN/°C).

In the bolted joint, the interface friction can transfer the internal forces of structural members, but during force transfer the distribution of interface friction in the splice plates is not uniform and more specifically, the interface frictions in the two-end areas (S_1 and S_{10}) are higher than the interface frictions in the middle areas (S_6 and S_7). Therefore, there is one decrease of linear slope in S_6 (0.92 kN/°C) and S_7 (0.83 kN/°C) and one increase of linear slope in S_{10} (2.43 kN/°C), as shown in Fig. 11(a). Furthermore, the linear slope relates to the shear capacity provided by group bolts. The decrease of linear slope in S_6 and S_7 makes the interface frictions smaller and has a wider margin to reach the shear capacity of group bolts in S_6 and S_7, while the increase of linear slope in S_{10} makes the interface friction closer to the shear capacity of group bolts in S_{10}.

Besides, Fig. 11(b) shows that the constant contains some positive and negative values, such as 0.54 kN/°C for S_4 and -0.28 kN/°C for S_2. These values are produced from the simulation error. Theoretically, these values should be 0 kN because they correspond to the interface friction without temperature increase. But the simulated data from finite element analysis are not totally the same with the theoretical values, so the constant $c(S_i)$ is not 0 kN after fitting the simulation data using Equation (1). What should be mentioned is that as the uniform temperature increases, the interface friction from $k(S_i)T$ is significantly higher than that from $c(S_i)$, so the influence of constant $c(S_i)$ can be reasonably ignored compared with $k(S_i)T$.
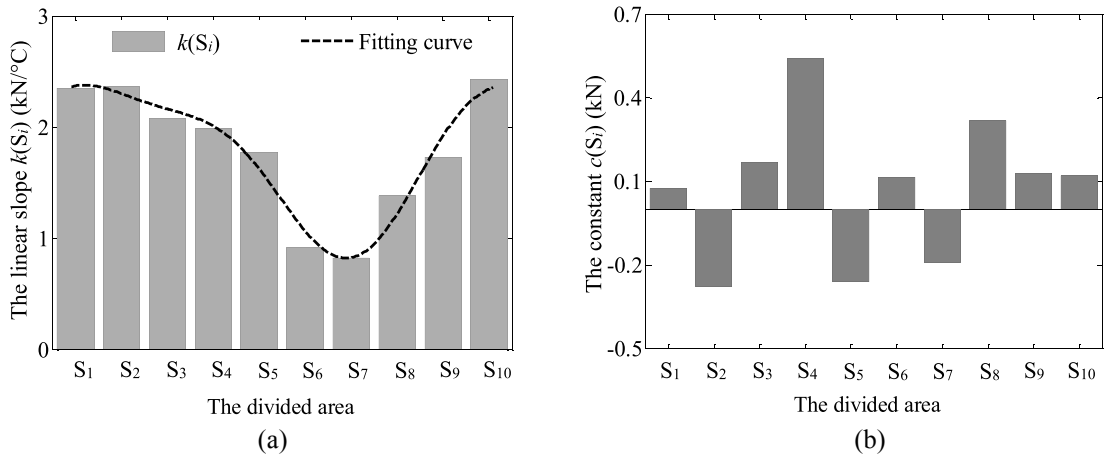
Figure 11. The linear slopes and constants in different divided areas. (a) The linear slope $k(S_i)$. (b) The constant term $c(S_i)$.

Furthermore, the distribution of linear slopes in different areas is mathematically described by one second-order of Fourier Series as follows:

$$k(S_i) = a_0 + \sum_{n=1}^{2} a_n \cos(\omega n i) + \sum_{n=1}^{2} b_n \sin(\omega n i) \qquad (2)$$

where $k(S_i)$ denotes the linear slope in the area S_i; ω, a_0, a_1, a_2, b_1 and b_2 are the Fourier coefficients. Using the least square method, the fitting curve of linear slopes is shown in Fig. 11(a), which agrees with the histograms of

linear slopes. The estimated values of ω, a_0, a_1, a_2, b_1 and b_2 are 0.6807, 1.736, 0.1261, 0.197, 0.7165, and 0.197, respectively. Furthermore, the distribution of interface frictions in different areas is mathematically formulated by $k(S_i)$ times T as follows:

$$f(S_i, T) = (a_0 + \sum_{k=1}^{2} a_k \cos(\omega ki) + \sum_{k=1}^{2} b_k \sin(\omega ki))T \tag{3}$$

THE EFFECT OF BOLT FRACTURE

This section thoroughly studies the effect of bolt fracture on the behaviour of high-strength bolted frictional steel connection, including the influence of quantity and location of fractured bolts on the interface friction as well as the linear superposition law of interface friction.

The influence factors: the quantity and location of fractured bolts

The quantity and location of fractured bolts can cause the redistribution of interface friction. However, a certain quantity of friction-type high-strength bolts may fracture in many possible locations, so it is difficult to consider all the possible fractured locations. Therefore, the random selection method is introduced here. In this method, the possible fractured locations are stochastically selected from the plate A. In detail, the interface friction caused by a certain quantity of fractured bolts in the random positions is treated as one random variable, and the mathematical expectation of random variable is used to describe the average influence of random fractured locations.

For example, suppose that 6 friction-type high-strength bolts are fractured in the divided area S_3, so their possible fractured locations are stochastically selected from area S_3 using the random selection method. In this method, the location of every bolt in the area S_3 is numbered from 1 to 8, and then 6 numbers are uniformly and randomly selected from the intervals [1, 8], which are treated as the fractured locations. Such selection process is repeated for 14 times, and finally 15 groups of possible fractured locations are stochastically selected. Through random selection analysis, the linear slopes of interface frictions for each group of fractured locations are obtained, and the mathematical expectation of these linear slopes is further calculated as shown in Figure 12. It can be seen that the mathematical expectation can well describe the average influence of random fractured locations, and the bolt fracture can obviously result in the redistribution of linear slope in S_3 by comparison with the one in Fig. 11(a); i.e., the linear slope in S_3 is obviously decreased from 2.08 kN/°C to 0.96 kN/°C after bolt fracture.

The clamping forces from bolts directly affect the interface friction, and the bolt fracture of some bolts in S_3 can directly result in the decrease of interface friction in this area and further result in the decrease of linear slope in the area S_3 from 2.08 kN/°C to 0.96 kN/°C. Furthermore, the linear slope relates to the shear capacity provided by group bolts. The decrease of linear slope caused by bolt fracture in S_3 makes the interface friction smaller and has a wider margin to reach the shear capacity of group bolts in S_3. Besides, because of the bolt fracture in S_3, the interface friction in S_3 is relatively smaller than that in S_4; i.e., there is one increase of linear slope from S_3 (0.96 kN/°C) to S_4 (2.15 kN/°C). But the linear slope (2.15 kN/°C) in S_4 after bolt fracture does not change much by comparison with the linear slope (1.99 kN/°C) before bolt fracture (see Fig. 11(a)), so there is no obvious change in the linear slope and has little effect on the group bolts in S_4.
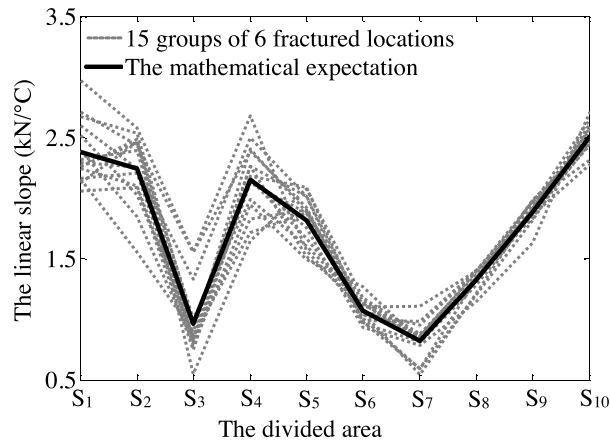
Figure 12. The influence of selected fractured locations.

Furthermore, different quantities of fractured bolts in the area S_3 are simulated, which are hypothetically 0, 2, 4, 6, and 8, respectively. Considering that the locations of fractured bolts in the area S_3 are uncertain, 15 groups of possible fractured locations for each quantity of fractured bolts are stochastically selected from the area S_3 using the random selection method. Finally, the mathematical expectation of linear slope for each certain quantity of fractured bolts is shown in Figure 13. It can be seen that the bolt fracture can seriously decrease the linear slopes in the bolt-fractured area S_3; i.e., the increasing quantity of fractured bolts from 0 to 8 can result in the decreasing linear slopes from 2.08 kN/°C to 0.22 kN/°C, but the fractured bolts in S_3 do not distinctly influence the linear slopes in the other areas.
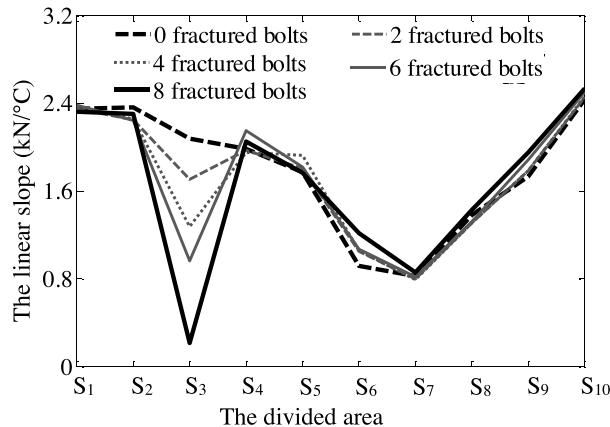

Figure 13. The mathematical expectation of linear slopes.

Then, the correlations between the linear slopes after bolt fracture and the linear slopes before bolt fracture are plotted in Figure 14. It can be seen that these correlations are clearly divided into two zones: in zone A, one obvious linear characteristics exists; in zone B, there are no any linear characteristics. Considering that the linear slopes in the zone B are all from area S_3, they are specially selected and their correlations with the fractured quantity are shown in Figure 15. It can be seen that, for this time, the correlation presents good linear characteristics, and the linear slope is linearly decreasing as the fractured quantity is increasing; i.e., increasing fractured bolts from 0 to 8 can result in decreasing linear slope from 2.08 kN/°C to 0.22 kN/°C.
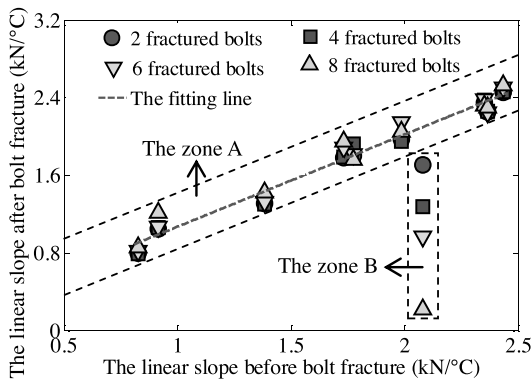
Figure 14. The correlations between linear slopes.
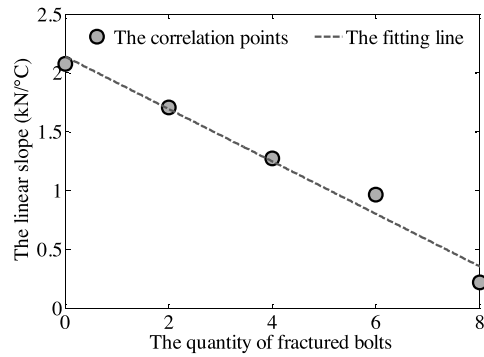
Figure 15. The correlation between linear slope and fractured quantity.

The linear characteristics in the zone A is mathematically described by one linear equation as follows:

$$K(S_i, N(S_3))=l(S_3)k(S_i)+n(S_3) \quad (i \ne 3) \tag{4}$$

where $K(S_i, N(S_3))$ denotes the linear slope of interface friction in the area S_i when the fractured quantity in the area S_3 is $N(S_3)$; $l(S_3)$ and $n(S_3)$ denote the coefficient term and constant term of linear equation regarding the bolt fracture in the area S_3, respectively; i denotes the serial number of divided area. The fitting line of linear characteristics in the zone A is shown in Figure 14, and the estimated values of $l(S_3)$ and $n(S_3)$ are 0.9035 and 0.2082, respectively.

The linear characteristics in the zone B is mathematically described by one linear equation as follows:

$$K(S_3, N(S_3))=p(S_3)N(S_3)+q(S_3) \tag{5}$$

where $K(S_3, N(S_3))$ denotes the linear slope of interface friction in the area S_3 when the fractured quantity in the area S_3 is $N(S_3)$; $p(S_3)$ and $q(S_3)$ denote the coefficient term and constant term of linear equation regarding the bolt fracture in the area S_3, respectively. The fitting line of linear characteristics in the zone B is shown in Figure 15, and the estimated values of $p(S_3)$ and $q(S_3)$ are -0.2231 and 2.141, respectively.

Overall, the linear slope of interface friction in the area S_i after bolt fracture is mathematically formulated by integrating Equation (4) into Equation (5) as follows:

$$K(S_i, N(S_3)) = \begin{cases} l(S_3)k(S_i)+n(S_3) & i \ne 3 \\ p(S_3)N(S_3)+q(S_3) & i = 3 \end{cases} \tag{6}$$

where $K(S_i, N(S_3))$ denotes the linear slope in the area S_i when the number of fractured bolts is $N(S_3)$ in the area S_3. Finally, the interface friction in the area S_i is mathematically described as follows:

$$f(S_i, N(S_3), T) = \begin{cases} l(S_3)k(S_i)T+n(S_3)T & i \ne 3 \\ p(S_3)N(S_3)T+q(S_3)T & i = 3 \end{cases} \tag{7}$$

where $f(S_i, N(S_3), T)$ denotes the interface friction in the area S_i when the temperature increase is T and the number of fractured bolts is $N(S_3)$ in the area S_3.

The linear superposition of interface friction

The friction-type high-strength bolts may fracture in different areas, and the fractured bolts in each area can cause the redistribution of interface friction. This part specifically studies whether the range of interface friction caused by fractured bolts in different areas can be calculated by summing together all the ranges of interface friction caused by fractured bolts in each area.

4 analytical cases are used in this study: in case I, no fractured bolts; in case II, 8 fractured bolts in the areas S_3 and S_4, respectively, namely, $N(S_3)=8$ and $N(S_4)=8$; in case III, 8 fractured bolts in the areas S_7 and S_8, respectively, namely, $N(S_7)=8$ and $N(S_8)=8$; in case IV, 8 fractured bolts in the areas S_3, S_4, S_7 and S_8, respectively, namely, $N(S_3)=8$, $N(S_4)=8$, $N(S_7)=8$ and $N(S_8)=8$. The linear slopes of interface frictions in cases I, II, III, and IV are, respectively, denoted as follows:

$$K_{case,I}=k(S_i) \tag{8a}$$

$$K_{case,II}=K(S_i, N(S_3)=8, N(S_4)=8) \tag{8b}$$

$$K_{case,III}=K(S_i, N(S_7)=8, N(S_8)=8) \tag{8c}$$

$$K_{case,IV}=K(S_i, N(S_3)=8, N(S_4)=8, N(S_7)=8, N(S_8)=8) \tag{8d}$$

where $K_{case,j}$ denotes the linear slope of interface friction in the case j, j=I, II, III, IV; $k(S_i)$ denotes the linear slope in the area S_i before bolt fracture; $K(S_i, N(S_3)=8, N(S_4)=8)$ denotes the linear slope in the area S_i with 8 fractured bolts in the areas S_3 and S_4, respectively; $K(S_i, N(S_7)=8, N(S_8)=8)$ denotes the linear slope in the area S_i with 8 fractured bolts in the areas S_7 and S_8, respectively; $K(S_i, N(S_3)=8, N(S_4)=8, N(S_7)=8, N(S_8)=8)$ denotes the linear slope in the area S_i with 8 fractured bolts in the areas S_3, S_4, S_7 and S_8, respectively. Finally, the finite element results of $K_{case,I}$, $K_{case,II}$, $K_{case,III}$ and $K_{case,IV}$ are shown in Figure 16. It can be seen that the fractured bolts in cases II, III, and IV can significantly decrease the linear slopes in the bolt-fractured areas by comparison with case I.
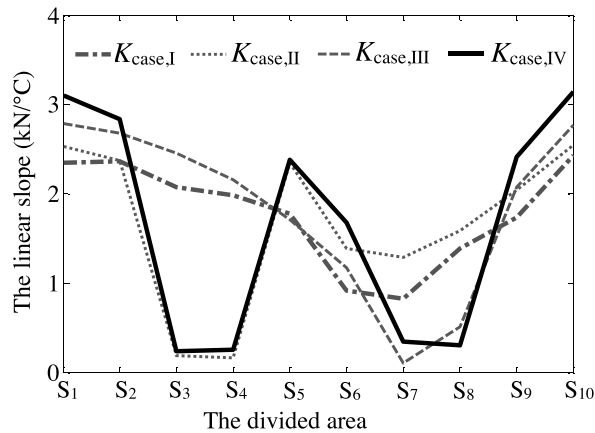

Figure 16. The results of $K_{case,I}$, $K_{case,II}$, $K_{case,III}$ and $K_{case,IV}$.

Compared with the linear slope without fractured bolts in the cases I, the ranges of linear slopes caused by fractured bolts in the cases II, III, and IV are, respectively, calculated as follows:

$$\Delta K_{case,II}=K_{case,II}-K_{case,I}=\Delta K(S_i, N(S_3)=8, N(S_4)=8)=K(S_i, N(S_3)=8, N(S_4)=8)-k(S_i) \tag{9a}$$

$$\Delta K_{case,III}=K_{case,III}-K_{case,I}=\Delta K(S_i, N(S_7)=8, N(S_8)=8)=K(S_i, N(S_7)=8, N(S_7)=8)-k(S_i) \tag{9b}$$

$\Delta K_{case,IV} = K_{case,IV} - K_{case,I} = \Delta K(S_i, N(S_3)=8, N(S_4)=8, N(S_7)=8, N(S_8)=8) = K(S_i, N(S_3)=8,$

$N(S_4)=8, N(S_7)=8, N(S_8)=8) - k(S_i)$ 　　　　　　　　　　　　　　(9c)

where $\Delta K_{case,k}$ denotes the range of linear slope in the case k, k=II, III, IV; $\Delta K(S_i, N(S_3)=8, N(S_4)=8)$ denotes the range of linear slope in the area S_i with 8 fractured bolts in areas S_3 and S_4, respectively; $\Delta K(S_i, N(S_7)=8, N(S_8)=8)$ denotes the range of linear slope in area S_i with 8 fractured bolts in areas S_7 and S_8, respectively; $\Delta K(S_i, N(S_3)=8, N(S_4)=8, N(S_7)=8, N(S_8)=8)$ denotes the range of linear slope in the area S_i with 8 fractured bolts in areas S_3, S_4, S_7 and S_8, respectively.

The calculation results of $\Delta K_{case,II}$, $\Delta K_{case,III}$ and $\Delta K_{case,IV}$ are shown in Figure 17, which present obvious decrease of linear slopes in the bolt-fractured areas. Moreover, considering that $\Delta K_{case,IV}$ is subject to the influence factors $N(S_3)=8$, $N(S_4)=8$, $N(S_7)=8$ and $N(S_8)=8$ and the sum of $\Delta K_{case,II}$ and $\Delta K_{case,III}$ is also subject to the same influence factors, the sum of $\Delta K_{case,II}$ and $\Delta K_{case,III}$ is further calculated as shown in Figure 17. It can be seen that $\Delta K_{case,II} + \Delta K_{case,III}$ and $\Delta K_{case,IV}$ have similar trends by comparison.

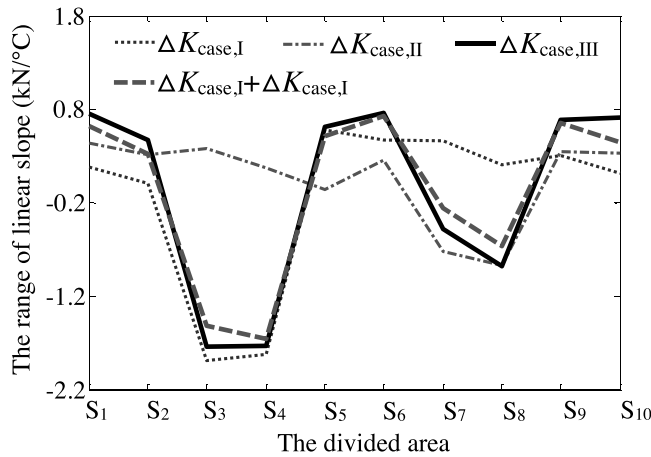**Figure 17.** The range of linear slopes in different areas.

Furthermore, the correlation between $\Delta K_{case,II} + \Delta K_{case,III}$ and $\Delta K_{case,IV}$ plotted in Figure 18 shows good linear characteristics, which is mathematically described by one linear equation as follows:

$\Delta K_{case,IV} = c_1(\Delta K_{case,II} + \Delta K_{case,III}) + C$ 　　　　　　　　　　　　(10)

where c_1 and C are the coefficient term and constant term of linear equation, respectively. Using least square method, the fitting line of linear characteristics is shown in Figure 18, where the estimated values of c_1 and C for the fitting line are 1.038 and 0.00769, respectively. It can be found that c_1 is close to 1, indicating that $\Delta K_{case,IV}$ can be treated as equal to the linear superposition of $\Delta K_{case,II}$ and $\Delta K_{case,III}$; i.e., the range of linear slope ($\Delta K_{case,IV}$) caused by fractured bolts in areas S_3, S_4, S_7 and S_8 can be calculated by linearly summing together the range of linear slopes ($\Delta K_{case,II}$) caused by fractured bolts in the areas S_3, S_4 and the range of linear slopes ($\Delta K_{case,III}$) caused by fractured bolts in the areas S_7, S_8.
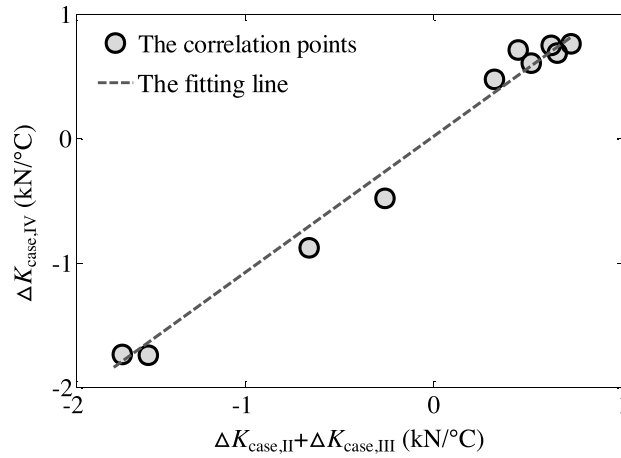
Figure 18. The correlation between $\Delta K_{\text{case,II}} + \Delta K_{\text{case,III}}$ and $\Delta K_{\text{case,IV}}$.

MATHEMATICAL MODELLDING ANALYSIS

This section will mathematically model the redistribution of linear slope caused by fractured bolts. First, the influence of fractured bolts in each area is modelled, and then the influence of fractured bolts in different areas is modelled using the linear superposition law of interface friction.

Modelling the influence of fractured bolts in each area

Equation (6) has revealed the influence of fractured bolts in the area S_3. By referring to Equation (6), the redistribution of linear slope caused by fractured bolts in any area S_j can be mathematically formulated as follows:

$$K(S_i, N(S_j)) = \begin{cases} l(S_j)k(S_i) + n(S_j) & i \neq j \\ p(S_j)N(S_j) + q(S_j) & i = j \end{cases} \tag{11}$$

where $K(S_i, N(S_j))$ denotes the linear slope of interface friction in the area S_i when the number of fractured bolts is $N(S_j)$ in the area S_j; $l(S_j)$, $p(S_j)$, $n(S_j)$ and $q(S_j)$ are the coefficient terms and constant terms of linear equations regarding the bolt fracture in the area S_j, respectively; i and j denote the serial numbers of divided area, respectively.

Ten analytical cases are used to estimate the values of coefficient terms and constant terms. In the kth case, all the fractured bolts are in the area S_k, where $k=1, 2, ..., 10$. Consider that the fractured bolts have many possible fractured quantities and locations, so 46 groups of possible fractured quantities and locations in each case are considered. In detail, the quantity of fractured bolts in each case is hypothetically 0, 2, 4, 6, and 8, respectively, and 15 groups of possible fractured locations for each certain number of fractured bolts are stochastically selected using the random selection method. Then, the results of ten cases are substituted into Equation (11), and the values of $l(S_j)$, $p(S_j)$, $n(S_j)$ and $q(S_j)$ are shown in Figure 19 after least square estimation. It can be seen that all the fitting values of $l(S_j)$ are close to 1, and the fitting values of $q(S_j)$ are similar with the linear slopes before bolt fracture in Fig. 11(a).
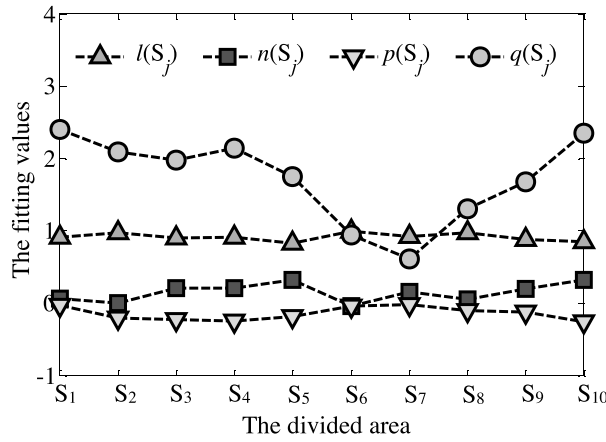
Figure 19. The fitting values of $l(S_j)$, $n(S_j)$, $p(S_j)$ and $q(S_j)$.

Another analytical case is used to verify whether the mathematical results from Equation (11) agree with the numerical result from finite element model. In this case, suppose that all the friction-type high-strength bolts in the area S_8 are fractured, and the numerical and mathematical results of linear slopes are shown in Figure 20. It can be seen that the numerical and mathematical results have similar trends, indicating that Equation (11) can well describe the redistribution of linear slope caused by fractured bolts in each divided area. Moreover, the range of linear slope caused by fractured bolts in any area S_j is calculated by $K(S_i, N(S_j))$ minus $k(S_i)$ as follows:

$$\Delta K(S_i, N(S_j)) = \begin{cases} l(S_j)k(S_i) + n(S_j) - k(S_i) & i \neq j \\ p(S_j)N(S_j) + q(S_j) - k(S_i) & i = j \end{cases} \quad (12)$$
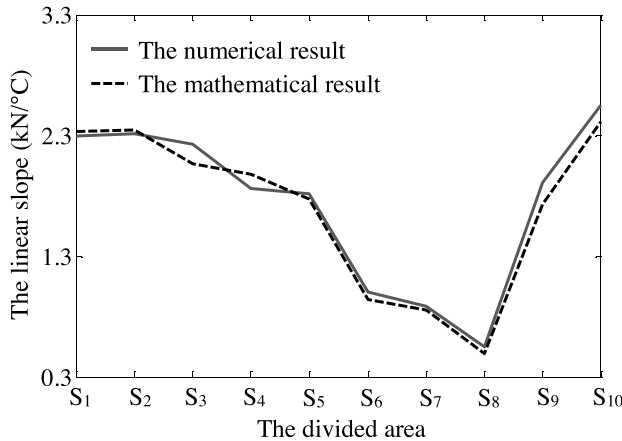

Figure 20. The numerical and mathematical results.

Modelling the influence of fractured bolts in different areas

The friction-type high-strength bolts may fracture in different areas. Equation (10) indicates that the influence of fractured bolts in each area can be linearly summed together, so the range of linear slopes caused by fractured bolts in different areas can be calculated by linearly summing together all the ranges of linear slopes caused by fractured bolts in each area as follows:

$$\Delta K(S_i, N(S_1), N(S_2), N(S_3), N(S_4), N(S_5), N(S_6), N(S_7), N(S_8), N(S_9), N(S_{10})) = c_1 \Delta K(S_i, N(S_1))$$
$$+ c_2 \Delta K(S_i, N(S_2)) + \ldots + c_{10} \Delta K(S_i, N(S_{10})) + C \quad (13)$$

Equation (13) is one multivariate linear regression equation. In this equation, $\Delta K(S_i, N(S_1), N(S_2), N(S_3), N(S_4), N(S_5), N(S_6), N(S_7), N(S_8), N(S_9), N(S_{10}))$ denotes the range of linear slope in the area S_i when the number of fractured bolts is $N(S_1)$ in the area S_1, $N(S_2)$ in the area S_2, $N(S_3)$ in the area S_3, $N(S_4)$ in the area S_4, $N(S_5)$ in the area S_5, $N(S_6)$ in the area S_6, $N(S_7)$ in the area S_7, $N(S_8)$ in the area S_8, $N(S_9)$ in the area S_9 and $N(S_{10})$ in the area S_{10}; $\Delta K(S_i, N(S_j))$ denotes the range of linear slope in the area S_i when the number of fractured bolts is $N(S_j)$ in the area S_j, $j=1, 2, ..., 10$; $c_1, c_2, ..., c_{10}$ are the regression coefficients; C is constant.

The regression coefficients and constant are unknown, so another ten analytical cases are used to estimate the values of regression coefficients and constant. In the kth case, all the bolts in the areas $S_1, S_2, ..., S_k$ are fractured, $k=1, 2, ..., 9$; in the tenth case, all the bolts in the areas $S_2, S_3, ..., S_{10}$ are fractured. The finite element results of $\Delta K(S_i, N(S_1), N(S_2), N(S_3), N(S_4), N(S_5), N(S_6), N(S_7), N(S_8), N(S_9), N(S_{10}))$, $\Delta K(S_i, N(S_1))$, $\Delta K(S_i, N(S_2))$, ..., $\Delta K(S_i, N(S_{10}))$ in ten cases are substituted into Equation (13), and after multivariate linear regression analysis, the estimated values of regression coefficients and constant are finally shown in Figure 21. It can be seen that all the regression coefficients are close to 1 and the constant is close to 0, verifying that the range of linear slopes caused by fractured bolts in different areas can be calculated by linearly summing together all the ranges of linear slopes caused by fractured bolts in each area.
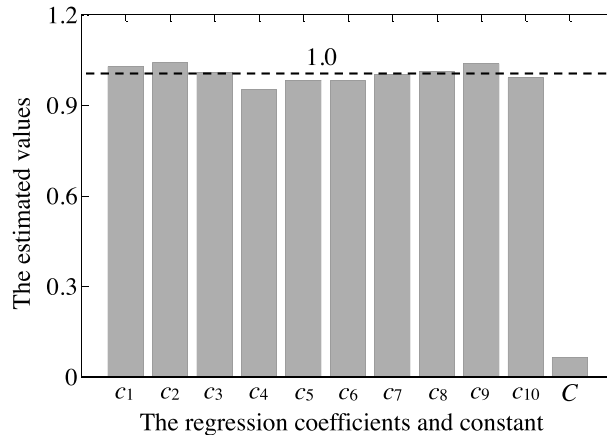

Figure 21. The estimated values of regression coefficients and constant.

Furthermore, the linear slope of interface friction caused by fractured bolts in different areas is mathematically formulated by the range of linear slope in Equation (13) plus $k(S_i)$ as follows:

$$K(S_i, N(S_1), N(S_2), N(S_3), N(S_4), N(S_5), N(S_6), N(S_7), N(S_8), N(S_9), N(S_{10}))=\Delta K(S_i, N(S_1),$$
$$N(S_2), N(S_3), N(S_4), N(S_5), N(S_6), N(S_7), N(S_8), N(S_9), N(S_{10}))+ k(S_i) \quad (14)$$

where $K(S_i, N(S_1), N(S_2), N(S_3), N(S_4), N(S_5), N(S_6), N(S_7), N(S_8), N(S_9), N(S_{10}))$ denotes the linear slope in the area S_i when the number of fractured bolts is $N(S_1)$ in the area S_1, $N(S_2)$ in the area S_2, $N(S_3)$ in the area S_3, $N(S_4)$ in the area S_4, $N(S_5)$ in the area S_5, $N(S_6)$ in the area S_6, $N(S_7)$ in the area S_7, $N(S_8)$ in the area S_8, $N(S_9)$ in the area S_9 and $N(S_{10})$ in the area S_{10}.

Finally, the redistribution of interface friction caused by fractured bolts in different areas is mathematically formulated by the linear slope in Equation (14) times uniform temperature T as follows:

$$f(S_i, N(S_1), N(S_2), N(S_3), N(S_4), N(S_5), N(S_6), N(S_7), N(S_8), N(S_9), N(S_{10}), T)=\Delta K(S_i, N(S_1),$$
$$N(S_2), N(S_3), N(S_4), N(S_5), N(S_6), N(S_7), N(S_8), N(S_9), N(S_{10}))T+ k(S_i)T \quad (15)$$

where $f(S_i, N(S_1), N(S_2), N(S_3), N(S_4), N(S_5), N(S_6), N(S_7), N(S_8), N(S_9), N(S_{10}), T)$ denotes the interface friction

in the area S_i when the temperature increase is T and the number of fractured bolts is $N(S_1)$ in the area S_1, $N(S_2)$ in the area S_2, $N(S_3)$ in the area S_3, $N(S_4)$ in the area S_4, $N(S_5)$ in the area S_5, $N(S_6)$ in the area S_6, $N(S_7)$ in the area S_7, $N(S_8)$ in the area S_8, $N(S_9)$ in the area S_9 and $N(S_{10})$ in the area S_{10}. What should be noted is that $f(S_i, N(S_1), N(S_2), N(S_3), N(S_4), N(S_5), N(S_6), N(S_7), N(S_8), N(S_9), N(S_{10}))$ is the mathematical expectation of interface friction caused by multiple stochastic fractured bolts. For example, $f(S_i, N(S_1)=4, N(S_2)=0, N(S_3)=0, N(S_4)=0, N(S_5)=0, N(S_6)=0, N(S_7)=0, N(S_8)=0, N(S_9)=0, N(S_{10}))=0$ is the mathematical expectation of interface friction caused by 4 fractured bolts in many possible fractured locations of area S_1.

Model validation

The linear slope of interface friction is treated as analytical indicator to validate the mathematical model. Supposing that the bolts in the areas S_3 and S_4 are all fractured, the numerical and mathematical results are shown in Figure 21, presenting similar trends. Moreover, 100 analytical cases are used to validate the mathematical model. In each case, the fractured bolts are uniformly and randomly selected from the area $p_1p_{11}q_{11}q_1$ in Figure 9. In detail, there are total 80 fractured bolts in the area $p_1p_{11}q_{11}q_1$, so the quantity of fractured bolts in each case is uniformly and randomly selected from the quantity interval [1, 80]; then the location of every bolt in the area $p_1p_{11}q_{11}q_1$ is numbered from 1 to 80, and the locations of a certain quantity of fractured bolts are uniformly and randomly selected from the location interval [1, 80].

After random selection analysis, the correlation between numerical and mathematical results of linear slopes is shown in Figure 22, presenting obvious linear characteristics. Furthermore, their correlation is further fitted by one linear equation as shown in Figure 22, where the estimated coefficient and constant of linear equation are 0.9723 and 0.0783, respectively. It can be found that the coefficient term is close to 1 and the constant term is close to 0, indicating that the mathematical model can well describe the redistribution of interface friction caused by fractured bolts.
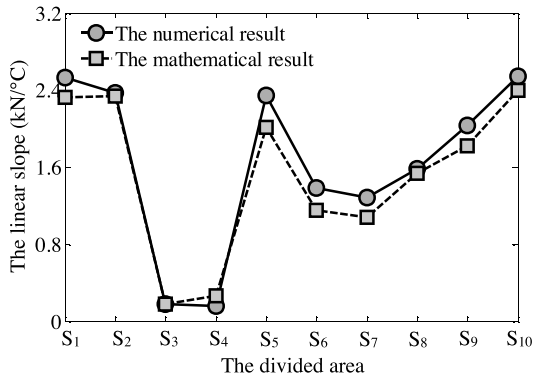

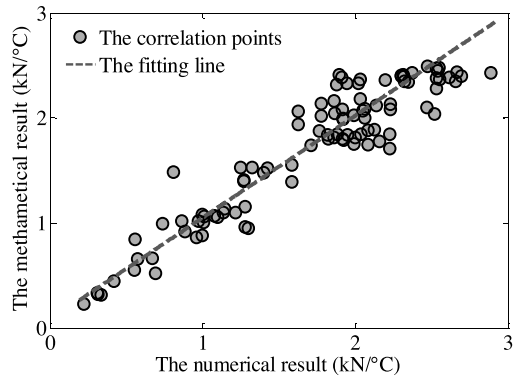**Figure 22.** The numerical and mathematical results.

Figure 23. The correlation between numerical and mathematical results.

MAIN RESULTS

This research carried out finite element analysis on the redistribution of interface friction in the high-strength bolted frictional steel connection under the effect of bolt fracture and uniform temperature field using LSDYNA. Main results with their indications are drawn as follows:

* The linear slopes in the splice plate are all positive, and the maximum and minimum values are 0.83 kN/°C and 2.43 kN/°C, respectively, indicating that increasing temperature can result in increasing interface friction in the splice plate;

* Linear slope directly relates to the interface friction, and lower linear slope means lower interface friction in the splice plates. The linear slopes in the splice plate gradually decrease from S_1 (2.35 kN/°C) to S_7 (0.83 kN/°C) and then gradually increase from S_7 (0.83 kN/°C) to S_{10} (2.43 kN/°C), indicating that the interface frictions in the two-end areas

are higher than the interface frictions in the middle areas;

* The bolt fracture can seriously decrease the linear slopes in the bolt-fractured area. The increasing quantity of fractured bolts from 0 to 8 in the area S_3 can result in obvious decreasing linear slopes from 2.08 kN/°C to 0.22 kN/°C;

* In the multivariate linear regression equation, the regression coefficients are close to 1 and the constant is close to 0, indicating that the range of linear slopes caused by fractured bolts in different areas can be calculated by linearly summing together all the ranges of linear slopes caused by fractured bolts in each area.

CONCLUSION AND RECOMMENDATION

In the bolted joint, the interface friction can transfer the internal forces of structural members. But during force transfer, the distributions of interface friction in the splice plates are not uniform, and furthermore, the bolt fracture can result in the redistribution of interface friction. To briefly sum up, increasing temperature means increasing interface friction; lower linear slope means lower interface friction; increasing fractured bolts means decreasing linear slope; the range of linear slopes caused by fractured bolts in different areas can be calculated by linearly summing together all the ranges of linear slopes caused by fractured bolts in each area.

In this research, the effect of the quantity and location of fractured bolts on the redistribution of interface friction is innovatively revealed. And furthermore, one new mathematical model is put forward to describe the redistribution of friction redistribution. By comparison with current studies without considering the redistribution of interface friction after bolt fracture, our research can provide useful reference for the behaviour study of friction-type high-strength bolted joint after bolt fracture.

However, this work primarily focused on the linear behavior of frictional steel connection, while the nonlinear behaviour was not taken into consideration. With regard to the plate sliding analysis and plastic deformation analysis, the nonlinear behavior should be taken into consideration, which deserves further study in our next research.

ACKNOWLEDGEMENTS

REFERENCES

Ali, B., Abdelwaheb, A., Abderahim, T. & Noureddine, B. 2012. Effect of contact forces on fretting fatigue behavior of bolted plates: Numerical and experimental analysis. Tribology International, **48**(2012): 237-245.

Bednarz, E.T. & Zhu, W.D. 2014. Identifying magnitudes and locations of loads on slender beams with welded and bolted joints using strain gauge-based force transducers with application to a portable army bridge. Computer-aided Civil and Infrastructure Engineering, **19**(2): 254–265.

Carlos, J.P., Reza, H.T., Barbara, R. & Dimitri D. 2017. Investigations on the fretting fatigue failure mechanism of bolted joints in high strength steel subjected to different levels of pre-tension. Tribology International, **108**(207): 128-140.

Chul, M.Y. & Shirley, J. Dyke. 2015. Vision-based automated crack detection for bridge inspection. Journal of Bridge Engineering, **30**(2015): 759–770.

Chakherlou, T.N., Rezavi, M.J. & Abazadeh B. 2013. Finite element investigations of bolt clamping force and friction coefficient effect on the fatigue behavior of aluminum alloy 2024-T3 in double shear lap joint. Engineering Failure Analysis, **29**: 62-74.

Delgado, J.M.D., Butler, L.J., Brilakis, I., Elshafie, M.Z.E.B. & Middleton, C.R. 2018. Structural Performance Monitoring Using a Dynamic Data-Driven BIM Environment, Journal of Computing in Civil Engineering, **32**(3): 324064504. https://doi.org/10.1061/(ASCE)CP.1943-5487.0000749.

Ding, Y.L., Wang, G.X., Hong, Y. & Song, Y.S. 2017. Detection and localization of degraded truss members in a steel arch bridge

based on correlation between strain and temperature. Journal of Performance of Constructed Facilities, **31**(5): 04017082. DOI: 10.1061/(ASCE)CF.1943-5509.0001075.

GB/T 1231-2006. 2006. Specifications of high strength bolts with large hexagon head, large hexagon nuts and plain washers for steel structures, Beijing: the Standards Press of China. (in Chinese)

Ju, M. & Oh, H. 2016. Static and fatigue performance of the bolt-connected structural jointed of deep corrugated steel plate member. Advances in Structural Engineering, **19**(9): 1435–1445.

Janne, J., Arto, L. & Antti, M. 2016. Experimental and numerical investigation of fretting fatigue behavior in bolted joints. Tribology International, **103**(2016): 440-448.

Jin, H. 2013. Discussion on maintenance method of Beijing-Shanghai High-speed Railway of Nanjing Dashengguan Changjiang River Bridge, Modern Transportation Technology, **10**(6): 51-55. (in Chinese)

Song, Z., Zhang, Z.J., Jiang, Y. & Zhu, J. 2018. Wind turbine health state monitoring based on a Bayesian data-driven approach, Renewable Energy, **125**: 172-181.

Wang, G. X. & Ding, Y. L. 2015. Research on monitoring temperature difference from cross sections of steel truss arch girder of Dashengguan Yangtze Bridge, International Journal of Steel Structures, **15**(3): 647-660.

Wang, G.X., Ding, Y.L., Song, Y.S., Wu, L.Y., Yue, Q. & Mao G.H. 2016. Detection and location of the degraded bearings based on monitoring the longitudinal expansion performance of the main girder of the Dashengguan Yangtze Bridge, Journal of Performance of Constructed Facilities, **30**(4): 04015074.

Xiao, J.Z. & Tong, X. 2012. Particle stratification and penetration of a linear vibrating screen by the discrete element method, International Journal of Mining Science and Technology, **22**(3): 357-362.

آثار درجة الحرارة المنتظمة وكسر البراغي على سلوك وصلة الصلب الملولبة عالية الصلابة من النوع الاحتكاكي في جسر سكك حديد داشنجوان

*جاوكسين وانغ و**يوليانج دينج

*مختبر الدولة الرئيسي للميكانيكا الجيولوجية والهندسة العميقة تحت الأرض، جامعة الصين للتعدين والتكنولوجيا، سوزهو، الصين

**المختبر الرئيسي للإنشاءات الخرسانية والخرسانة المسبقة الإجهاد التابعة لوزارة التعليم، جامعة جنوب شرق، نانجينغ، الصين

الخلاصة

يمكن أن يتسبب كسر البراغي للمفصل الملولب عالي الصلابة من النوع الاحتكاكي في إعادة توزيع الاحتكاك البيني، مما قد يعرض سلامة وصلات الهياكل الإنشائية إلى أخطار جسيمة. ومع ذلك، بالكاد تركز الدراسات الحالية على إعادة توزيع الاحتكاك البيني بعد كسر البراغي. ولذلك، يعمل هذا البحث على تحليل العناصر المحدودة بشأن إعادة توزيع الاحتكاك البيني الناجم عن البراغي المكسورة. أولاً، تم استخدام نموذج العناصر المحدودة للمفصل الملولب عالي الصلابة من النوع الاحتكاكي لدراسة الاختلافات في الاحتكاك البيني تحت درجات حرارة موحدة وكذلك توزيع الاحتكاك البيني في مناطق مختلفة. علاوة على ذلك، تم تقديم طريقة اختيار عشوائية لشرح كيفية كمية وموقع البراغي المكسورة على إعادة توزيع الاحتكاك البيني. وأخيراً، تم تصميم نموذج رياضي لإعادة توزيع الاحتكاك لوصف إعادة توزيع الاحتكاك البيني في وصلة الصلب الملولب عالي الصلابة من النوع الاحتكاكي بعد كسر البراغي. بعد التحقق من فاعلية النموذج الرياضي، فيمكنه أن يصف إعادة توزيع الاحتكاك البيني الناجم عن البراغي المكسورة بشكل جيد.